CERN-PH-TH/2004-030
IFT-2004/15
hep-ph/0403180
**February 1, 2008**



# Patterns of Lepton-Flavour Violation Motivated by Decoupling and Sneutrino Inflation

**Piotr H. Chankowski**[1], **John Ellis**[2], **Stefan Pokorski**[1], **Martti Raidal**[3] and **Krzysztof Turzyński**[1]

[1] Institute of Theoretical Physics, Warsaw University, Hoża 69, 00-681, Warsaw, Poland
[2] Theoretical Physics Division, Physics Department, CERN, CH-1211 Geneva 23, Switzerland
[3] National Institute of Chemical Physics and Biophysics, Tallinn 10143, Estonia

**Abstract**

We present predictions for flavour-violating charged-lepton decays induced by the seesaw mechanism implemented within the constrained minimal supersymmetric standard model (CMSSM) with universal input soft supersymmetry breaking terms. We assume that one heavy singlet neutrino almost decouples from the see-saw mechanism, as suggested by the pattern of light neutrino masses and mixing angles. This is suggested independently by sneutrino inflation with a low reheating temperature, $T_{RH} \lesssim 10^7\,\mathrm{GeV}$, so as to avoid overproducing gravitinos. This requirement further fixes the mass of the weakly-coupled sneutrino, whose decays may lead to leptogenesis. We find that $BR(\mu \to e\gamma) \gtrsim 10^{-13}$ but $BR(\tau \to \mu\gamma) \lesssim 10^{-9}$ in the bulk of the acceptable parameter space, apart from a few isolated points. The ratio $BR(\mu \to e\gamma)/BR(\tau \to e\gamma)$ depends on only one complex parameter, and is particularly interesting to compare with experiment.

# 1 Introduction

The observation of neutrino mixing [1] has led many authors to consider the possibility of flavour violation and CP violation in the charged-lepton sector [2]. The most predictive framework for such studies is the seesaw model for neutrino masses [3] implemented within the minimal supersymmetric extension of the Standard Model, constrained to have universal soft supersymmetry breaking terms at some input renormalization scale characteristic of grand unification (CMSSM). This framework allows one to explore the possible links between lepton-flavour violation (LFV), neutrino oscillations and leptogenesis [4, 5], assuming the cosmological baryon asymmetry to have originated from CP-violating decays of heavy singlet neutrinos and their supersymmetric partners.

Even the minimal three-generation seesaw model contains 18 free parameters [6, 7], in addition to those describing supersymmetry breaking. Four combinations of these seesaw parameters have been determined by neutrino-oscillation experiments, two mixing angles and two mass-squared differences. More of the seesaw parameters may be determined by low-energy neutrino experiments, but not all of them, and specifically not all those controlling leptogenesis [8, 9, 10, 11, 12]. Under these circumstances, supplementary hypotheses are needed if one is to make unambiguous predictions for LFV, leptonic CP violation and leptogenesis. Fortunately, one can find good physical motivation for certain simplifying assumptions. The observed hierarchy of differences in neutrino masses-squared can be interpreted as a hierarchy in the masses themselves. Such a pattern of the active neutrino masses together with the measured nearly bi-maximal neutrino mixing would be naturally explained if one of the heavy singlet neutrinos is almost decoupled from the seesaw mechanism [13, 14]. As we analyze in this paper, this decoupling hypothesis imposes important constraints on the seesaw parameters, and hence leads to interesting predictions for LFV processes.

The decoupling hypothesis is supported by the suggestion that the scalar field supposed to be responsible for inflation, the inflaton, is one of the heavy singlet sneutrinos [15]. Requiring a low reheating temperature, $T_{RH} \lesssim 10^7$ GeV after inflation, in order to solve the cosmological gravitino problem [16], forces the inflaton sneutrino to couple very weakly to ordinary matter and its superpartner almost to decouple from the seesaw mechanism. In order to explain simultaneously the duration of the inflationary epoch responsible for the large-scale structures observed in the Universe and the magnitudes of the perturbations observed in the cosmic microwave background, the mass of this sneutrino should be around $2 \times 10^{13}$ GeV [17]. This is well inside the range thought plausible in the seesaw model. Also, as discussed elsewhere, sneutrino inflation makes predictions for cosmic microwave background (CMB) observables, such as the scalar spectral index and the ratio of tensor to scalar perturbations [17], which are consistent with data on the CMB and cosmological structure formation [18].

It is striking that, on the one hand, naturalness arguments for models of neutrino masses and mixings and, on the other hand, the hypothesis of the sneutrino inflation, both motivate independently a similar pattern in the seesaw mechanism.

The scenario with the heaviest right-chiral neutrino decoupled is a natural possibility. However, a hierarchy of the heavy singlet neutrino masses could be compensated by some hierarchy in the neutrino Yukawa couplings, and it is interesting to consider also the decoupling of one of the lighter neutrinos. In fact, decoupling of the lightest singlet neutrino was considered in the sneutrino inflation model of [17], but one may also consider inflation driven by one of the heavier sneutrinos, if it is decoupled. The purpose of this paper is to outline the different scenarios for decoupling one of the heavy singlet neutrinos, and explore in some detail the LFV signature of some specific examples.

We discuss our different decoupling assumptions for the neutrino Yukawa couplings in Section 2, and explore their various predictions for LFV decays in Section 3. For each case we also discuss the possible leptogenesis, which is necessarily nonthermal in the sneutrino inflation models with low reheating temperature, with the CP asymmetry generated in the decays of the inflaton [19]. As we discuss in Section 3, the details of this mechanism depend on which neutrino plays the role of the inflaton.

The main result of our investigations is that the decoupling hypothesis leads to relatively rigid predictions for the branching ratios $BR(\ell_i \to \ell_j \gamma)$. For most of the acceptable parameter range, we predict $BR(\mu \to e\gamma) \gtrsim 10^{-13}$, within the reach of the experiment now underway at PSI. However, for generic models with $BR(\mu \to e\gamma)$ below the present experimental upper limit, we find that $BR(\tau \to \mu\gamma) < 10^{-9}$, apart from very particular parameter points, which may be of special theoretical interest. Only in these cases might $BR(\tau \to \mu\gamma)$ be within the reach of present experiments at $B$ factories and the LHC. The ratios $BR(\ell_i \to \ell_j \gamma)/BR(\ell_k \to \ell_m \gamma)$ depend, within our assumptions, on only one unknown complex parameter that appears in the neutrino Yukawa couplings. If possible, a measurement of $BR(\tau \to \mu\gamma)/BR(\mu \to e\gamma)$ would provide particularly interesting information on complex structure in the seesaw model.

## 2 Decoupling Assumptions for Yukawa Couplings

In the seesaw mechanism the observed neutrino masses and mixing are determined by the neutrino Yukawa couplings $\mathbf{Y}_\nu^{AB}$ and the mass matrix $\mathbf{M}_R$ of the heavy singlet neutrinos. The mass matrix of the light left-chiral neutrinos is given by:

$$(\mathbf{m}_\nu)_{AB} = \langle H \rangle^2 \mathbf{C}_{AB} \tag{1}$$

where $\langle H \rangle$ is the electroweak symmetry breaking vacuum expectation value of the relevant Higgs doublet and the complex symmetric matrix $\mathbf{C}$ is the coefficient of the dimension-five operator $\mathcal{L}_{\rm eff} = -\mathbf{C}_{AB}(L_A H)(L_B H)/2$ resulting from integrating out heavy right-chiral neutrinos [3]. The matrix $\mathbf{C}$, which can be diagonalized by a unitary matrix $\mathbf{U}_\nu^T \mathbf{C} \mathbf{U}_\nu = \mathrm{diag}(c_1^2, c_2^2, c_3^2)$, is at the high scale given by

$$\mathbf{C} = -\mathbf{Y}_\nu^T \mathbf{M}_R^{-1} \mathbf{Y}_\nu \ . \tag{2}$$

Similarly as for the quark sector, the number of observables in the light neutrino sector is smaller than the number of free parameters in $\mathbf{Y}_\nu$ and $\mathbf{M}_R$. Indeed, even in the basis in which $\mathbf{M}_R = \mathrm{diag}(M_1, M_2, M_3)$ and $\mathbf{Y}_e = \mathrm{diag}(y_e, y_\mu, y_\tau)$, the most general solution of the relation (2) for $\mathbf{Y}_\nu$ reads:

$$\mathbf{Y}_\nu^{AB} = i M_A^{1/2} \sum_C \mathbf{\Omega}_{AD} c_D \mathbf{U}_\nu^{BD*} \ . \tag{3}$$

A complex orthogonal matrix $\mathbf{\Omega}$ accounts for the six-parameter ambiguity in translating the 3 neutrino masses and 6 parameters in $\mathbf{U}_\nu$ into the 15 parameters of the neutrino Yukawa coupling $\mathbf{Y}_\nu$ [6]. Thus, even assuming that the elements of the mixing matrix $\mathbf{U}_\nu$ are determined with sufficient accuracy, the predictions of the CMSSM for flavour-violating processes in the lepton sector depend on several unknown factors: the pattern of the light neutrino masses (hierarchical, inversely hierarchical or degenerate), the right-chiral neutrino masses $M_A$ and on the matrix $\mathbf{\Omega}$. In practice, one should also remember that the Majorana phases in $\mathbf{U}_\nu$ may never be measured.

In a large number of papers, the predictions for the charged lepton decays have been discussed under various specific assumptions about those unknown factors [6, 7, 8, 9, 10, 20, 21, 22, 23, 24, 25, 26, 27, 28, 29]. In the present paper we re-examine the predictions for the charged lepton decays of the CMSSM under two very general assumptions. We assume the hierarchy in mass for both, left- and right-chiral neutrinos

$$\begin{aligned} m_{\nu_1} \ll m_{\nu_2} \leq m_{\nu_3} \\ M_1 \leq M_2 < M_3 \end{aligned} \tag{4}$$

We take $m_{\nu_3} = \sqrt{\Delta m^2_{\rm atm}} = 0.05$ eV, $m_{\nu_2} = \sqrt{\Delta m^2_{\rm sol}} = 0.008$ eV and the neutrino mixing matrix in the form:

$$\mathbf{U}_\nu = \begin{pmatrix} c_{12} & s_{12} & s_{13} e^{-i\delta} \\ -\frac{s_{12}}{\sqrt{2}} + \ldots & \frac{c_{12}}{\sqrt{2}} + \ldots & \frac{1}{\sqrt{2}} \\ \frac{s_{12}}{\sqrt{2}} + \ldots & -\frac{c_{12}}{\sqrt{2}} + \ldots & \frac{1}{\sqrt{2}} \end{pmatrix} \cdot \mathrm{diag}(e^{i\phi_1}, e^{i\phi_2}, 1) \tag{5}$$

where $s_{12}^2 \equiv \sin^2\theta_{12} = 0.315$, the dots stand for small terms $\sim \mathcal{O}(s_{13})$ (for the sake of definiteness we have assumed that $0 < \theta_{23} < \pi/2$). For the $\mathbf{U}_\nu^{13}$ entry we use the two scenarios specified in Table 1. We do not assume any particular values of the Majorana phases $\phi_1$ and $\phi_2$, but treat them as free parameters. It is important to note that, for hierarchical light neutrino masses, renormalization effects on the mass eigenvalues and on the mixing angles, in particular, are small and can be neglected (see e.g. [30, 31]). Thus one can use the measured $\mathbf{U}_\nu$ in (3).

It has frequently been observed that the simultaneous appearance of hierarchical light neutrino masses and two large mixing angles is not 'natural' in the seesaw mechanism (see e.g. [14]). Important exceptions are so-called sequential neutrino dominance models with one neutrino decoupled [13, 24] or even absent [32, 33, 26, 34]. Otherwise some particularities, as found, e.g., in models with horizontal symmetries [35, 36, 37], are

| case | $\lvert\mathbf{U}_\nu^{13}\rvert$ | $\arg \mathbf{U}_\nu^{13}$ |
|---|---|---|
| a) | 0 | – |
| b) | 0.1 | $-\pi/2$ |

Table 1: *Selected values of* $\mathbf{U}_\nu^{13}$ *at the electroweak scale used in the analysis.*

necessary. This motivates our second assumption that one singlet right-chiral neutrino, not necessarily the heaviest one, decouples from the seesaw mechanism, in the sense that at most one neutrino, say $N_A$, contributes to the mass $m_{\nu_1}$ of the lightest neutrino. As has been explained in [38, 39], for $\mathbf{Y}_\nu^{A2}/M_A \to 0$ and $\mathbf{Y}_\nu^{A3}/M_A \to 0$ the matrix $\mathbf{\Omega}$ in (3) has to be, depending on the index $A$, of one of the following three forms:

$$\text{decoupling of } N_1 \qquad \mathbf{\Omega} = \begin{pmatrix} 1 & 0 & 0 \\ 0 & z & p \\ 0 & \mp p & \pm z \end{pmatrix} \tag{6}$$

$$\text{decoupling of } N_2 \qquad \mathbf{\Omega} = \begin{pmatrix} 0 & z & p \\ 1 & 0 & 0 \\ 0 & \mp p & \pm z \end{pmatrix} \tag{7}$$

$$\text{decoupling of } N_3 \qquad \mathbf{\Omega} = \begin{pmatrix} 0 & z & p \\ 0 & \pm p & \mp z \\ 1 & 0 & 0 \end{pmatrix} \tag{8}$$

where $z^2 + p^2 = 1$. Since $\mathbf{\Omega}_{AB}^2$ determines directly the contribution of the right-chiral neutrino $N_A$ to the mass of the light neutrino $\nu_B$ [24], the assumption that $N_A$ effectively decouples means that it is only $N_A$ that contributes to $m_{\nu_1}$, and that it does not contribute to $m_{\nu_{2,3}}$. In the limit of strict decoupling, in which $\mathbf{Y}_\nu^{AB}/M_A \to 0$ for $B = 1, 2, 3$, the lightest left-chiral neutrino is massless because, as follows from (6)-(8) and (3), $\sqrt{m_{\nu_1}} \propto (\mathbf{Y}_\nu \mathbf{U}_\nu)^{A1}/\sqrt{M_A}$. Of course, in realistic cases the zeroes in $\mathbf{\Omega}$ are non-zero numbers $\ll 1$. The stability of the patterns (6)-(8) with respect to radiative corrections is analyzed in the Appendix.

Another motivation for seesaw models with the light-neutrino masses dominated by two heavy singlet neutrinos follows from the hypothesis that the cosmological inflaton field is one of the heavy sneutrinos, $\tilde{N}_A$, say. As has been discussed in [17], in order to reproduce the measured characteristics of the CMB in such a scenario, and to agree with the data on the cosmological structure formation, the inflaton-sneutrino and its superpartner, the right-chiral neutrino $N_A$ must have a mass $M_A \simeq 2 \times 10^{13}\,\text{GeV}$. The reheating temperature following inflaton decay is

$$T_{RH} \sim \sqrt{\tilde{m}_A M_P}\frac{M_A}{\langle H \rangle}, \tag{9}$$

where

$$\tilde{m}_A \equiv \left(\mathbf{Y}_\nu \mathbf{Y}_\nu^\dagger\right)_{AA} \langle H \rangle^2 / M_A = \sum_{B=1}^{3} |\mathbf{\Omega}_{AB}|^2 m_{\nu_B} \ . \tag{10}$$

For $M_A \simeq 2\times 10^{13}$ GeV, it follows from (9) that one needs $\tilde{m}_A \lesssim 10^{-17}$ eV in order to obtain $T_{RH} \lesssim 10^7$ GeV [40]. This in turn enforces a pattern in the $\mathbf{\Omega}$ matrix with $(1,0,0)$ in the $A$'th row. Thus reheating temperature $T_{RH}$ after inflation that is low enough to solve the cosmological gravitino problem is possible in sneutrino inflation scenarios provided the neutrino partner of the $\tilde{N}_A$ inflaton (not necessarily the heaviest one) decouples from the seesaw mechanism. The possibility of explaining the baryon asymmetry of the Universe through leptogenesis following inflation with the patterns (6)-(8) will be discussed in Sec. 3.

The three patterns of $\mathbf{\Omega}$ shown in (6), (7) and (8) provide distinctly different realizations of the seesaw mechanism. However, as we explain later, they give similar predictions for LFV decays in a large range of parameter space. It follows that the predictions for neutrino masses and mixings and for LFV are invariant under certain transformations on the neutrino Yukawa matrix. Therefore, even with all possible data on neutrino masses and mixings, as well as on LFV processes that can (in principle) be obtained experimentally, the bottom-up approach can determine $\mathbf{Y}_\nu$ only up to these transformations.

The analysis presented in this paper is based only on the general assumptions described above. It is, however, worth commenting on the link of such a bottom-up approach to model-dependent (top-down) studies based on specific 'theories' of the neutrino Yukawa matrix and of the masses of the heavy singlet neutrinos, based for example on texture zeroes. Once such a theory of flavour is specified in some electroweak basis, as in [39, 26] for example, $\mathbf{\Omega}$ can be read off easily from (3), by first performing the necessary field rotations diagonalizing the heavy singlet neutrino mass matrix and the charged lepton Yukawa coupling matrix. One may envisage a situation in which the electroweak basis in which the flavour theory predicts texture zeroes in $\mathbf{Y}_\nu$ is only slightly different from the basis in which our assumptions are formulated, i.e., the matrices $\mathbf{Y}_e$ and $\mathbf{M_R}$ are almost diagonal. The equation (3) fixes then the value of the parameter $z$ in terms of the ratios of some elements of $\mathbf{U}_\nu$ and of $m_{\nu_2}/m_{\nu_3}$. Indeed, for the pattern (6) [pattern (7), (8)], $\mathbf{Y}_\nu^{1A}$ [$\mathbf{Y}_\nu^{2A}$, $\mathbf{Y}_\nu^{3A}$] can be neglected, and if in addition the texture gives $\mathbf{Y}_\nu^{2B} = 0$ [$\mathbf{Y}_\nu^{1B} = 0$] for $B = 2, 3$ then one obtains from (3)

$$\pm\, z = 1 - \frac{1}{2}\frac{m_{\nu_2}}{m_{\nu_3}}\left(\frac{\mathbf{U}_\nu^{B2*}}{\mathbf{U}_\nu^{B3*}}\right)^2 \approx 1 \mp 0.06 e^{-2i\phi_2}\ . \tag{11}$$

Similarly, if $\mathbf{Y}_\nu^{3B} = 0$ [$\mathbf{Y}_\nu^{3B} = 0$, $\mathbf{Y}_\nu^{2B} = 0$] for $B = 2, 3$ because of texture zeroes, then

$$z = \pm\sqrt{\frac{m_{\nu_2}}{m_{\nu_3}}}\frac{\mathbf{U}_\nu^{B2*}}{\mathbf{U}_\nu^{B3*}} \approx \pm 0.3 e^{-i\phi_2}\ . \tag{12}$$

For a diagonal matrix $\mathbf{M}_R$, the solutions (12) and (11) remain approximately valid if

$$|\mathbf{U}_\ell^{AB}| \lesssim \sqrt{\frac{m_{\ell_A}}{m_{\ell_B}}} \quad \text{for} \quad A < B, \tag{13}$$

where $\mathbf{U}_\ell$ is the matrix diagonalizing $\mathbf{Y}_e^\dagger \mathbf{Y}_e$. The solution (11) is more sensitive to departures of $\mathbf{M}_R$ from the diagonal form than is (12). It will be useful to remember these particular qualitative patterns with $z \approx 0.3$ or $z \approx 1$ in our subsequent analysis.

# 3 Implications of Decoupling for LFV Decays

In this Section we first present the general background for calculating the branching ratios for the LFV decays $l_A \to l_B\gamma$ and then discuss in detail the predictions that follow from the pattern (6) of the matrix $\mathbf{\Omega}$. The predictions following from the two other patterns are similar and will require only a short discussion. For each of the patterns we also discuss possible scenarios for leptogenesis.

## 3.1 General Formalism

The branching ratios for LFV decays are well described by a single-mass-insertion approximation [20, 24]:

$$BR(l_A \to l_B\gamma) \approx \frac{\alpha^3}{G_F^2}\mathcal{F}(m_0, M_{1/2}, \mu)|\tilde{\mathbf{m}}^2_{L_{AB}}|^2 \tan^2\beta, \tag{14}$$

where $\mathcal{F}$ is a function of the soft supersymmetry-breaking masses fixed at the high scale $M_X$. The ratio $f(m_0, M_{1/2}) \equiv \mathcal{F}(m_0, M_{1/2})/\mathcal{F}(100\text{ GeV}, 500\text{ GeV})$ for $\tan\beta = 10$ and $\mu > 0$ is shown Fig. 1a. The reference values $m_0 = 100$ GeV, $M_{1/2} = 500$ GeV are chosen for their consistency with the astrophysical cold dark matter constraint [41]. In the subsequent figures, we show predictions with the factor $f(m_0, M_{1/2})$ removed, and Fig. 1a can be used to obtain the corresponding predictions for other values of $m_0, M_{1/2}$.

The off-diagonal entries in the slepton mass matrix $\tilde{\mathbf{m}}^2_L$ are generated radiatively by the renormalization-group (RG) evolution from $M_X$ to the electroweak scale. In the commonly-used approximation of using only a single recurrence in solving the relevant RGEs, they are related to the neutrino Yukawa couplings by

$$\tilde{\mathbf{m}}^2_{L_{AB}} = \kappa \sum_C (\mathbf{Y}_\nu^{CA})^*(\Delta t + \Delta\ell_C)\mathbf{Y}_\nu^{CB}, \tag{15}$$

where $\kappa = -6m_0^2 - 2A_0^2$, $\Delta t = \ln(M_X/M_3)/16\pi^2$, $\Delta\ell_C = \ln(M_3/M_C)/16\pi^2$ [42]. This result is not very accurate, as we demonstrate in Fig. 1b, where we show the ratio of (15) to $\tilde{\mathbf{m}}^2_{L_{AB}}$ as obtained by solving numerically the one-loop RGEs. Although the results presented in this paper are based on the exact numerical integration of the RGEs with successive decoupling of the singlet neutrinos at the appropriate scales, we note that the numerical result is well approximated by the following correction to $\kappa$:

$$\begin{aligned}\Delta\kappa = \Big[&-\frac{36}{5}g^2(2M_{1/2}^2 + 3m_0^2 + A_0^2 + 2A_0M_{1/2}) \\ &+y_t^2(36m_0^2 + 24A_0^2) + (6m_0^2 + 12A_0^2)\mathsf{Tr}(\mathbf{Y}_\nu^\dagger\mathbf{Y}_\nu)\Big]\,\Delta t,\end{aligned} \tag{16}$$

where the top-quark Yukawa $y_t$ and the other couplings are taken at the scale $M_X$. The correction (16) is obtained by including the second recurrence in solving the RGEs. However, the approximation (15) is sufficient for the qualitative discussion of our results.

Combining (15) with (3) and (4) and using one of the decoupling scenarios (6)-(8), one may obtain formulae for the decay rates $BR(l_A \to l_B\gamma)$. It is useful to discuss first the results obtained under the technical assumption that the hierarchies of neutrino masses obey

$$\begin{array}{ll} m_{\nu_3} M_2 < m_{\nu_2} M_3 & \text{for pattern (6)}, \\ m_{\nu_3} M_1 < m_{\nu_2} M_3 & \text{for pattern (7), or} \\ m_{\nu_3} M_1 < m_{\nu_2} M_2 & \text{for pattern (8)}, \end{array} \tag{17}$$

where the inequality signifies a ratio of at least a factor 2 or 3. We study deviations from (17) at the end of Subsection 3.2. As follows from eq. (3), under these assumptions and for generic values of the $z$ and $p$ parameters, the formula (15) is well approximated by the contribution of the product $(\mathbf{Y}_\nu^{3A})^* \mathbf{Y}_\nu^{3B}$ for the structures (6) and (7), and of the product $(\mathbf{Y}_\nu^{2A})^* \mathbf{Y}_\nu^{2B}$ for the structure (8). Nevertheless, for the sake of the future discussion, in the formulae given below we display also the nonleading contribution to the formula (15). In our numerical calculation we keep, of course, complete $\tilde{\mathbf{m}}^2_{L_{AB}}$ obtained by solving the RGEs.

## 3.2 The Decoupling of $N_1$ and LFV Decays

With the pattern (6), the mass insertion $\tilde{\mathbf{m}}^2_{L_{32}}$ relevant for $\tau \to \mu\gamma$ reads:

$$\begin{aligned} \tilde{\mathbf{m}}^2_{L_{32}} \;\approx\; & \kappa \frac{m_{\nu_3} M_3 \Delta t}{\langle H \rangle^2} \times \\ & \Big[ \mathbf{U}_\nu^{33} \mathbf{U}_\nu^{23*} \left( |z|^2 + S|1-z^2| \right) + R\, \mathbf{U}_\nu^{33} \mathbf{U}_\nu^{22*} \left( S z \sqrt{1-z^2}^{\,*} - z^* \sqrt{1-z^2} \right) + \\ & + R\, \mathbf{U}_\nu^{32} \mathbf{U}_\nu^{23*} \left( S z^* \sqrt{1-z^2} - z \sqrt{1-z^2}^{\,*} \right) + R^2\, \mathbf{U}_\nu^{32} \mathbf{U}_\nu^{22*} \left( S|z|^2 + |1-z^2| \right) \Big], \end{aligned} \tag{18}$$

where $R = \sqrt{m_{\nu_2}/m_{\nu_3}} \sim 0.41$ and $S = M_2(1+\Delta\ell_2/\Delta t)/M_3 \sim M_2/M_3$ gives the subleading contribution of the product $(\mathbf{Y}_\nu^{2A})^* \mathbf{Y}_\nu^{2B}$. The branching ratio does not depend strongly on the masses $M_1$ and $M_2$ and the Majorana phase $\phi_1$, as long as $M_1 < M_2 \ll M_3$, i.e., for $S \ll 1$. For the results presented below, we take $M_3 = 5 \times 10^{14}$ GeV, $M_2 = 3 \times 10^{13}$ GeV ($S \approx 0.1$) and $M_1 = 2 \times 10^{13}$ GeV, consistent with inflation being driven by the lightest singlet sneutrino. Our choice of $M_3$ makes $\mathbf{Y}_\nu^{3A}$ naturally of order of unity. Moreover, due to maximal atmospheric neutrino mixing, $\mathsf{Re}(\mathbf{U}_\nu^{33}\mathbf{U}_\nu^{22*} - \mathbf{U}_\nu^{32}\mathbf{U}_\nu^{23*}) \sim \mathcal{O}(s_{13})$ and the real parts of the second and third term in (18) cancel each other almost completely. Then it is only $\mathsf{Im}(\tilde{\mathbf{m}}^2_{L_{32}})$ which depends on the Majorana phase $\phi_2$, and the branching ratio $BR(\tau \to \mu\gamma) \propto |\tilde{\mathbf{m}}^2_{L_{32}}|^2$ consist of a sum of two positive terms: a constant one and a term which oscillates with $\phi_2$ as $\sin^2[\phi_2 - \arg(z^*\sqrt{1-z^2})]$. The relative magnitude of these two terms depends on the phase of $z$, and a non-zero value of $\mathbf{U}_\nu^{13}$ adds a slight modulation proportional to $-\sin(\phi_2 - \arg(z^*\sqrt{1-z^2}))$.

This behaviour is clearly seen in Fig. 2, which shows $BR(\tau \to \mu\gamma)$ as a function of $\phi_2$ for $|z|^2 = 1/2$, $\tan\beta = 10$ and $A_0 = 0$, for the two different values of the $\mathbf{U}_\nu^{13}$ element

specified in Table 1. As already mentioned, the values of the branching ratio for other values of $m_0$ and $M_{1/2}$ can be obtained by appropriate rescalings that can be read off from Fig. 1a. The dependence of $BR(\tau \to \mu\gamma)$ on $|z|$ is depicted in Fig. 3. For each value of $|z|$, the maximal and minimal predictions for this branching ratio are shown. In particular, the allowed range for $|z|^2 = 1/2$ corresponds to a horizontal squeezing of Fig. 2.

At this point, it is worth summarizing the dependence of $BR(\tau \to \mu\gamma)$ on the model parameters. The dependence on $|z|$ gives a factor that varies by $10^4$ for $|z|$ changing between 0.01 and 1.4. As can be seen in Fig. 1a, for $m_0$ and $M_{1/2}$ varying in the range 100 GeV$\to$1 TeV, the decay rate can change by another a factor of roughly $10^4$. Furthermore, the dependence of (14) on $\tan^2\beta$ brings in also a factor of order a few to $\sim 10^3$. One should also remember the quadratic dependence of $BR(\tau \to \mu\gamma)$ on $M_3$. The fact that $\phi_2$ is inaccessible to experiment introduces only a small additional uncertainty of the order of factor 4.

Collecting all this information, we see that, under the present assumptions and with the anticipated experimental sensitivity down to $BR(\tau \to \mu\gamma) \sim 10^{-9}$, this decay can in the scenario (6) be experimentally accessible for a large range of parameters. The question which part of this parameter space can be consistent with the present experimental bound $BR(\mu \to e\gamma) < 1.2 \times 10^{-11}$ is considered below. It is however worth noting that, assuming that the soft masses and $\tan\beta$ can be determined by other measurements with sufficient precision, the measurement of this decay would, owing to the strong dependence on $|z|$: $BR(\tau \to \mu\gamma) \propto |z|^4$, provide a relatively narrow range of $|z|$ for fixed masses of the heavy singlet neutrinos.

The quantities $\tilde{\mathbf{m}}^2_{L_{21}}$ relevant for $\mu \to e\gamma$ and $\tilde{\mathbf{m}}^2_{L_{31}}$ relevant for $\tau \to e\gamma$ can be approximated by:

$$\tilde{\mathbf{m}}^2_{L_{A1}} \approx \kappa \frac{m_{\nu_3} M_3 \Delta t}{\langle H \rangle^2} \left[ R \mathbf{U}^{A3}_\nu \mathbf{U}^{12*}_\nu \left( S z \sqrt{1-z^2}^* - z^* \sqrt{1-z^2} \right) \right.$$
$$\left. + R^2 \mathbf{U}^{A2}_\nu \mathbf{U}^{12*}_\nu \left( S|z|^2 + |1-z^2| \right) + \mathbf{U}^{A3}_\nu \mathbf{U}^{13*}_\nu \left( |z|^2 + S|1-z^2| \right) \right], \qquad (19)$$

where we have dropped the terms suppressed by both $\mathbf{U}^{13}_\nu$ and $R$. For the sake of qualitative discussion, the third term can always be neglected (for $\mathbf{U}^{13}_\nu \neq 0$, this is a good approximation provided $|1-z^2|$ is not too close to zero). For $BR(\mu \to e\gamma)$, the factors depending on the neutrino masses and mixing in the first two terms in (19) can be estimated as:

$$R|\mathbf{U}^{23}_\nu \mathbf{U}^{12}_\nu| \sim 0.16 \qquad R^2|\mathbf{U}^{22}_\nu \mathbf{U}^{12}_\nu| \sim 0.05, \qquad (20)$$

whose ratio is $3.1 \pm 0.5$. For $S \ll 1$ the relative phase between the first two terms in (19) is $\phi_2 - \arg(z^*\sqrt{1-z^2}) + \pi$. This is clearly seen in Figs. 4a and 4b, where we show $BR(\mu \to e\gamma)/f(m_0, M_{1/2})$ as a function of the Majorana phase $\phi_2$ for $|z| = 1/\sqrt{2}$ and three representative values of $\arg z$. The strength of the $\phi_2$-dependent interference pattern seen in Fig. 4 varies with the values of $|z|$ and $\arg z$. In particular, it decreases both for $|z| \to 0$ and $|z| \gg 1$, where the second term in (19) dominates over the first one. Comparison of Fig. 4a with 4b shows that a non-zero value of $\mathbf{U}^{13}_\nu$ enhances the interference pattern but does not change it qualitatively.

The dependence of $BR(\mu \to e\gamma)$ on the other parameters is similar to that of $BR(\tau \to \mu\gamma)$. In Fig. 5 we show $BR(\mu \to e\gamma)$ as a function of $|z|$ for the same values of the other parameters as we used in Fig. 3 for $BR(\tau \to \mu\gamma)$. The comparison of Figs. 1 and 5 shows that, except for two special points at $|z| \sim 0.3$ and $|z| \sim 1$, the branching ratio of the decay $\mu \to e\gamma$ for $f(m_0, M_{1/2}) \gtrsim 1$ and $\tan\beta \gtrsim 10$ is above the experimental upper bound $1.2 \times 10^{-11}$. The minimum of $BR(\mu \to e\gamma)$ at $|z| \sim 0.3$ is due to the destructive interference of the first two terms in (19): for $S \ll 1$ they are of equal magnitude just for $|z| \sim 0.3$, and for any value of $\arg z$ the Majorana phase $\phi_2$ can be chosen so that these two terms approximately cancel each other. The minima for $|z| \sim 1$ are instead caused by the simultaneous vanishing of the two first terms in the limit $S = 0$. Therefore they appear only for $\arg z \approx 0$ and $\pi$. For $\mathbf{U}_\nu^{13} = 0$ the non-zero value of $BR(\mu \to e\gamma)$ at the single minimum seen in Fig. 5a is due to $S \neq 0$ in the second term in (19); for $\mathbf{U}_\nu^{13} \neq 0$ (Fig. 5b) there are two minima whose position is determined by the cancellation of the first and third terms in (19), which holds for $z \approx \pm(1 - \frac{1}{2}\alpha \exp(2i(\delta - \phi_2))$, where $\alpha = |\mathbf{U}_\nu^{13*}/R\mathbf{U}_\nu^{12*}| \approx 1/5$, i.e. for $|z| \approx 1 - \frac{1}{2}\alpha\cos(2(\delta - \phi_2))$. The minima of $BR(\mu \to e\gamma)$ occur at the values of $z$ corresponding to the texture zeroes (11) and (12). This is obvious for $\mathbf{Y}_\nu^{3A} = 0$, since $BR(l_A \to l_B\gamma) \propto |\mathbf{Y}_\nu^{3A*}\mathbf{Y}_\nu^{3B}|^2$, but it is a non-trivial result for $\mathbf{Y}_\nu^{22} = 0$, which follows from the structure of the masses and mixings of the light neutrinos.

As follows from Fig. 1, for $BR(\mu \to e\gamma)$ to be consistent with the experimental bound in a larger range of $|z|$ values, the gaugino mass $M_{1/2}$ at the high scale should be bigger than 500 GeV and/or $M_3$ significantly smaller than $5 \times 10^{14}$ GeV. On the other hand, $M_{1/2} \gtrsim 500$ GeV corresponds to third-generation masses above 1 TeV at the electroweak scale, which begins to conflict with the naturalness requirement. This conflict becomes even sharper for higher values of $\tan\beta$. This discussion suggests that, if $\mathbf{\Omega}$ is of the form (6), the rate of $\mu \to e\gamma$ decay should be close to the present experimental bound.

At this point, we can also address the question whether the present experimental bound $BR(\mu \to e\gamma) < 1.2 \times 10^{-11}$ allows for $BR(\tau \to \mu\gamma) \geq 10^{-9}$. This can best be discussed by studying the predictions for the ratio $BR(\mu \to e\gamma)/BR(\tau \to \mu\gamma)$, which depends only on $z$ and $\phi_2$, as the dependence on the soft supersymmetry-breaking parameters, $\tan\beta$ and $M_3$ cancel out. Furthermore, since $BR(\tau \to \mu\gamma)$ is a monotonic function of $|z|$ and can be changed by a factor of 10 at most by changing the Majorana phase $\phi_2$, the minima of the ratio $BR(\mu \to e\gamma)/BR(\tau \to \mu\gamma)$ follow the minima of $BR(\mu \to e\gamma)$. Maximal and minimal possible values of $BR(\mu \to e\gamma)/BR(\tau \to \mu\gamma)$ obtained by varying $\phi_2$ in the range $(0, 2\pi)$ are shown in Fig. 6 as a function of $|z|$ for three different values of $\arg z$.

As seen in Fig. 6, generically $BR(\mu \to e\gamma)/BR(\tau \to \mu\gamma) \sim 0.1$ to 1, that is $BR(\tau \to \mu\gamma) \lesssim 10^{-10}$ for $BR(\mu \to e\gamma) \lesssim 10^{-11}$. However, there are exceptions to this rule in a few isolated regions corresponding to the minima of $BR(\mu \to e\gamma)$ seen in Fig. 5. This means that observation of $\tau \to \mu\gamma$ at a rate $\gtrsim 10^9$ in future experiments would be a strong constraint for top-down models of neutrino masses and mixings.

Finally, we briefly consider the decay $\tau \to e\gamma$. The dependences of the predictions for $BR(\tau \to e\gamma)$ on the soft mass parameters $z$ and $\phi_2$ are similar to those of $BR(\mu \to e\gamma)$.

However, since the relative phase between $\mathbf{U}_\nu^{22}$ and $\mathbf{U}_\nu^{32}$ approximately equals $\pi$, for the value of $\phi_2$ for which $BR(\mu \to e\gamma)$ is minimized $BR(\tau \to e\gamma)$ is maximal and vice versa, as shown in Fig. 7. The dependence of $BR(\tau \to e\gamma)/BR(\tau \to \mu\gamma)$ is depicted in Fig. 8.

We have presented predictions obtained under the supplementary assumption (17). However, for $M_2$ close enough to $M_3$ but still reasonably smaller, the first condition (17) is no longer satisfied. It is therefore worthwhile to check the behaviour of the predictions for the decays rates when $M_2$ approaches $M_3$. In particular, one may wonder whether the deep minima in $BR(\mu \to e\gamma)$ at $|z| \sim 0.3$ and $|z| \sim 1$ are filled in by additional contributions to (15) coming from the product $(\mathbf{Y}_\nu^{2A})^* \mathbf{Y}_\nu^{2B}$, which may now be non-negligible. This is shown in Fig. 9. The two minima persist even for relatively large values of the mass ratio, $M_2/M_3 \lesssim 0.4$ for $\mathbf{U}_\nu^{13} = 0$ and $M_2/M_3 \lesssim 0.25$ for $|\mathbf{U}_\nu^{13}| = 0.1$, but the first minimum shifts to slightly higher values of $|z|$ for larger values of $M_2/M_3$.

In this Section we have discussed the results for $BR(l_A \to l_B\gamma)$ obtained under the hypothesis that the lightest right-chiral neutrino decouples from the seesaw mechanism. To a very good approximation, these results do not depend on the mass $M_1$. The particular value $M_1 = 2 \times 10^{13}$ GeV, is compatible with inflation driven by the lightest sneutrino. As analyzed in [17], succesful nonthermal leptogenesis with low reheating temperature can then occur. This is because for the zeroes in (6) representing small complex numbers it is easy to obtain values of the CP asymmetry parameter $\epsilon_1$ saturating the Davidson-Ibarra upper bound [43][1].

For any other value, $M_1 \neq 2 \times 10^{13}$ GeV but still with the pattern (6), some other field must be responsible for inflation. Disregarding the cosmological gravitino problem, one may then contemplate the possibility of conventional thermal leptogenesis. It turns out that, with zeroes in (6) representing small complex numbers, leptogenesis can be realized for $T_{RH} \gtrsim 10^9$ GeV [5, 45]. In both cases, the final lepton number asymmetry does not depend on the parameter $z$ of the $\mathbf{\Omega}$ matrix. The possibility of lowering the reheating temperature necessary for the thermal leptogenesis in a scenario with degenerate neutrinos $N_1$ (decoupled) and $N_2$ (not decoupled) remains an open question for the pattern (6).

### 3.3 LFV decays and the decoupling of $N_2$ or $N_3$.

The predictions for the LFV decays with the decoupling of $N_2$ [pattern (7)] or $N_3$ [pattern (8)] are easy to discuss if one remembers that $\tilde{\mathbf{m}}_{L_{AB}}^2$ in eq. (15) is dominated by the contribution of the product $(\mathbf{Y}_\nu^{3A})^* \mathbf{Y}_\nu^{3B}$ or $(\mathbf{Y}_\nu^{2A})^* \mathbf{Y}_\nu^{2B}$, respectively. This means that in the case (7) the predictions for the decay rates are the same as for pattern (6), for the same values of $\mathbf{Y}_\nu^{3A}$ and if in both cases the subleading contributions to $\tilde{\mathbf{m}}_{L_{AB}}^2$ are negligible [2]. For the decoupling of $N_3$, the predictions are the same as for the decoupling of $N_1$ if we

[1] However, for moderately hierarchical heavy neutrino masses it is possible to obtain larger values of the CP asymmetry than the abovementioned bound [44].

[2] Predictions in the two patterns are the same including the subleading effects if the $\mathbf{Y}_\nu^{1A}$ in the case (7) are numerically equal to the $\mathbf{Y}_\nu^{2A}$ in the case (6).

change $\mathbf{Y}_\nu^{3A} \to \mathbf{Y}_\nu^{2A}$ and keep the numerical values unchanged. At this point, it is worth recalling equation (3):

$$\begin{aligned}\mathbf{Y}_\nu^{3A} &= iM_3^{1/2}\left(\mathbf{\Omega}_{31}c_1\mathbf{U}_\nu^{A1*} + \mathbf{\Omega}_{32}c_2\mathbf{U}_\nu^{A2*} + \mathbf{\Omega}_{33}c_3\mathbf{U}_\nu^{A3*}\right)\\ \mathbf{Y}_\nu^{2A} &= iM_2^{1/2}\left(\mathbf{\Omega}_{21}c_1\mathbf{U}_\nu^{A1*} + \mathbf{\Omega}_{22}c_2\mathbf{U}_\nu^{A2*} + \mathbf{\Omega}_{23}c_3\mathbf{U}_\nu^{A3*}\right)\end{aligned} \tag{21}$$

We see that the predictions following from decoupling of $N_1$ and $N_2$ are, to a good approximation, identical for the same values of $M_3$. In particular, the mass of the decoupled neutrino can be kept at $2\times 10^{13}$ GeV (for sneutrino inflation) [3]. Decoupling of $N_3$ leads to the same LFV decay rates as decoupling of $N_1$ for $M_2$ replaced by a numerically equal $M_3$. Moreover, with $M_3 = 2\times 10^{13}\,\text{GeV}$ the dominant contribution to $\mathbf{Y}_\nu^{2A}$ in (21) comes from $M_2 < M_3$. So the $BR(l_A \to l_B\gamma)$ discussed in Section 3 are rescaled by the ratio $M_2^2/M_3^2$. Since, for (6), $M_3 \gg 2\times 10^{13}\,\text{GeV}$ and, for (8), $M_2 \ll M_3 = 2\times 10^{13}\,\text{GeV}$, the predictions for the decay rates are strongly suppressed in the latter case. We conclude that, if the heaviest right-chiral neutrino is the inflaton, the decays $l_A \to l_B\gamma$ are unlikely to be observed experimentally.

Let us now consider the possible types of leptogenesis with $N_2$ or $N_3$ decoupled. In nonthermal leptogenesis following sneutrino-driven inflation [17], the final lepton asymmetry is generated directly in the decay of the vacuum condensate of the sneutrino-inflaton field $\tilde{N}_2$ or $\tilde{N}_3$. Since the final lepton-number-to-entropy ratio $Y_L$ generated in this way is given by:

$$Y_L = \frac{3}{4}\epsilon_A\frac{T_{RH}}{M_{\text{infl}}}\ , \tag{22}$$

a low reheating temperature $T_{RH} \lesssim 10^7$ GeV and $M_{\text{infl}} = 2\times 10^{13}$ GeV require the CP asymmetry parameters $\epsilon_2$ or $\epsilon_3$, respectively, to assume values of the order of $\epsilon_{\text{ref}}/10$, where $\epsilon_{\text{ref}} = \frac{3M_{\text{infl}}m_{\nu_3}}{8\pi\langle H\rangle^2} \sim 4\times 10^{-3}$ (for $\tilde{N}_1$-driven inflation $\epsilon_{\text{ref}}$ is the same as the Davidson-Ibarra bound on $\epsilon_1$ [43]). In Table 2 we display the one-loop contributions to $\epsilon_A/\epsilon_{\text{ref}}\eta_{AE}$ from the individual virtual states $N_E$ (and $\tilde{N}_E$) [46], where

$$\eta_{AE} = \left|\frac{\sum_D m_{\nu_D}^2\,\mathsf{Im}\left[(\mathbf{\Omega}_{AD}\mathbf{\Omega}_{ED}^*)^2\right]}{m_{\nu_3}\sum_C m_{\nu_c}|\mathbf{\Omega}_{AD}|^2}\right| \leq \sum_D \frac{m_{\nu_D}}{m_{\nu_3}}|\mathbf{\Omega}_{ED}|^2 \tag{23}$$

For the pattern (7), only the contribution from $N_1$ is suppressed by the small value of $(M_1/M_2)^2$, whereas for the pattern (8) all the contributions are small. This suppression can only be overcome if $\eta_{AE}$, that is some $|\mathbf{\Omega}_{ED}|^2$, are large, which, recalling the interpretation of $\mathbf{\Omega}$ as the dominance matrix, means some fine-tuning in the seesaw mechanism. This can be seen in Figure 10, where we show in the form of a scatter plot the CP asymmetries $\epsilon_2$ and $\epsilon_3$ generated in the direct decays of the sneutrino-inflaton $\tilde{N}_2$ [$\tilde{N}_3$], relevant for the patterns (7) [(8)], respectively, as functions of the parameter $p = \sqrt{1-z^2}$ of the $\mathbf{\Omega}$ matrix. We have chosen $\arg p = \pi/4$ and $\arg\mathbf{\Omega}_{B2} = \arg\mathbf{\Omega}_{B3} = \pi/4$ for $B = 2, 3$ and scanned over $|\mathbf{\Omega}_{B2}|$ and $|\mathbf{\Omega}_{B3}|$ in the range $10^{-3}-10^{-1}$ with a uniform distribution over the

[3] With the exception that, in the case (7), subleading effects may become important only at the expense of lowering $M_3$, i.e., when the LFV decay rates are suppressed.

| | pattern (7) | pattern (8) |
|---|---|---|
| $E=1$ | $\frac{2M_1^2}{3M_2^2}\left(1+\ln\frac{M_1}{M_2}\right)$ | $\frac{2M_1^2}{3M_3^2}\left(1+\ln\frac{M_1}{M_3}\right)$ |
| $E=2$ | $---$ | $\frac{2M_2^2}{3M_3^2}\left(1+\ln\frac{M_2}{M_3}\right)$ |
| $E=3$ | 1 | $---$ |

Table 2: *Estimated maximal contributions to $|\epsilon_2/\epsilon_{\rm ref}\eta_{2E}|$ for the pattern (7) and to $|\epsilon_3/\epsilon_{\rm ref}\eta_{3E}|$ for the pattern (8), due to virtual $N_E$ exchange in the loop (see the text for explanation).*

logarithmic scale. It is clear from Figures 10a and 10b that, whilst the Davidson-Ibarra bound [43] can be saturated for the pattern (7) with $|z|, |p| \lesssim 1$, for the pattern (8) this is possible only for $|z|, |p| \gtrsim 3$ and, hence, requires fine tuning in the seesaw mechanism.

Finally, we can abandon the hypothesis of sneutrino-driven inflation and consider more conventional thermal leptogenesis with the patterns (7) and (8). The masses of all the three right-chiral neutrinos, including the decoupled one, can be then arbitrary. If they are split sufficiently for the final lepton number asymmetry to be generated entirely in the decays of the lightest right-chiral neutrino, the only relevant CP asymmetry parameter is $\epsilon_1$, which in both cases (7) and (8), takes the form

$$\epsilon_1 \approx -\frac{3M_1}{8\pi\langle H\rangle^2}\frac{\mathsf{Im}(z^2)\left(m_{\nu_3}^2-m_{\nu_2}^2\right)}{|z|^2 m_{\nu_2}+|1-z^2|m_{\nu_3}} \tag{24}$$

The important wash-out parameter $\tilde{m}_1$ then reads

$$\tilde{m}_1 \approx \left(|z|^2 m_{\nu_2}+|1-z^2|m_{\nu_3}\right)\ . \tag{25}$$

The basic consequences of (24) and (25) were explored in [38].[4] It was found that, because $\tilde{m}_1$ is bounded from below by $m_{\nu_2}$ and not by $m_{\nu_1}$, the wash-out processes are very efficient and successful leptogenesis requires compensation by a large $\epsilon_1$, i.e., large $M_1$. For the patterns (7) and (8), with $M_1 = 10^{11}$ GeV and $M_1 = 5\times 10^{11}$ GeV, regions of the plane $(|z|, \arg z)$ leading to successful thermal leptogenesis are shown in Fig. 11 [5]. The two panels of Fig. 11 correspond to the two cases specified in Table 1. Contours of constant $BR(\mu\to e\gamma)$ minimized with respect to $\phi_2$ are also shown. As can be seen, regions of the $(|z|, \arg z)$ plane where the thermal leptogenesis reproduces the observed baryon number asymmetry of the Universe and regions where the experimental bound on $BR(\mu\to e\gamma)$ can be respected overlap with each other. However, since $T_{RH} \gtrsim M_1 \gtrsim 10^{11}$ GeV for this mechanism to work, the cosmological gravitino problem has to solved in some other way, perhaps by the gravitino being the lightest supersymmetric particle [47] (see, however, [41]).

[4] In [38] only the decoupling of the heaviest right-chiral neutrino, i.e., the pattern (8), was considered explicitly. However, it is clear that these results apply to the pattern (7) as well.

[5] Recent advances in the calculation of the lepton number asymmetry [45] have been included.

As has been discussed in [38, 48, 49, 50, 51, 52], for the pattern (8) $T_{RH} \lesssim 10^6$ GeV can be obtained if $N_1$ and $N_2$ are tightly degenerate, with $1 - M_1/M_2 \lesssim 10^{-5}$. In this case, however, since $N_3$ is decoupled and $M_2 \lesssim 10^6$ GeV, branching ratios $BR(l_i \to l_j\gamma)$ are $\sim 10^{-18}$, too small to be accessible to current experiments. For the pattern (7), one of the two degenerate neutrinos would be the decoupled one, and to obtain succesful leptogenesis with $T_{RH} \lesssim 10^6$ GeV one would probably need the degeneracy of all the three right-chiral neutrinos. In this case the LFV decays would again be inaccessible.

# 4 Conclusions

We have calculated the branching ratios for the decays $l_A \to l_B\gamma$ in the MSSM under the assumption that the masses of both the light and heavy singlet neutrinos are hierarchical, and that one singlet neutrino (not necessarily the heaviest one) decouples from the seesaw mechanism. For each of the three possible realizations of the decoupling hypothesis we have also discussed possible leptogenesis scenarios.

The predictions for $BR(l_A \to l_B\gamma)$ do not depend on which neutrino decouples. To a very good approximation they depend on only one non-decoupled neutrino mass, the heavier one. Apart from the dependence on the soft mass terms and on $\tan\beta$, parameters that will hopefully be measured in other experiments, the branching ratios depend strongly on just one complex parameter $z$, which fixes all the relevant Yukawa couplings. Consequently, our two assumptions lead to relatively rigid predictions for the decay rates. For $m_0, M_{1/2} \lesssim 1\,\text{TeV}$ and $M_A \gtrsim 10^{13}\,\text{GeV}$, the decay rate for $\mu \to e\gamma$ is predicted to be close to the present experimental bound $1.2 \times 10^{-11}$, namely $BR(\mu \to e\gamma) \gtrsim 10^{-14}$. However, for $BR(\mu \to e\gamma) < 1.2 \times 10^{-11}$, the decay rate for $\tau \to \mu\gamma$ is generically below the anticipated experimental sensitivity $10^{-9}$, except for some special values of $|z|$. The ratios $BR(\mu \to e\gamma)/BR(\tau \to \mu\gamma)$ and $BR(\tau \to e\gamma)/BR(\tau \to \mu\gamma)$ depend on $z$ only, with the dependences on the other parameters cancelling out. These ratios would therefore be particularly interesting to compare with experiment.

**Acknowledgments**
P.H.Ch. was supported by the Polish State Committee for Scientific Research Grant 2 P03B 040 24 for 2003-2005 and the EC Contract HPRN-CT-2000-00152. He would also like to thank the CERN Theory Division for hospitality while writing the paper. The work of S.P. and K.T. was partially supported by the Polish State Committee for Scientific Research Grant 2 P03B 129 24 for 2003-2005 and the EC Contract HPRN-CT-2000-00148. The work of M.R. was supported by the ESF Grants 5135 and 5935 and by the EC MC contract MERG-CT-2003-503626. K.T. would like to thank the Michigan Center of Theoretical Physics and Theory Division at CERN, where parts of this work were done, for their hospitality and stimulating atmospheres.

# Appendix - Stability of the $\mathbf{\Omega}$ patterns

In bottom-up evolution, the Yukawa couplings $\mathbf{Y}_\nu^{1B}$, $\mathbf{Y}_\nu^{2B}$ and $\mathbf{Y}_\nu^{3B}$ enter into the RGEs for the soft slepton masses at the scales $M_1$, $M_2$ and $M_3$, respectively. We see from (3) that they are expressed at these respective scales in terms of the matrix $\mathbf{\Omega}$, which is taken to have one of the scale-independent forms (6)-(8). However, once the $\mathbf{Y}_\nu^{1B}$ (say) is fixed by (3) in terms of $\mathbf{\Omega}$ at the scale $M_1$, their scale dependences are controlled by the appropriate RGEs, and at the scale $M_2$ they do not satisfy the relation (3) with scale-independent $\mathbf{\Omega}$. Thus, fixing $\mathbf{Y}_\nu^{2B}$ at $M_2$ from (3) with a scale-independent orthogonal matrix $\mathbf{\Omega}$ is not a fully consistent procedure, as it distorts the relations between $\mathbf{Y}_\nu^{1B}$ and $\mathbf{Y}_\nu^{2B}$ which follow from the assumption that, e.g., with (6) $\mathbf{Y}_\nu^{1B}/M_1 \to 0$ for $B = 2, 3$.

We can get some control over the quality of this approximation in the following way. Suppose that all three right-chiral neutrinos are integrated out at a scale $Q_0$ chosen in such a way that the threshold corrections to the relation (2) vanish. It is easy to verify that in a one-loop approximation $M_1 < Q_0 < M_3$. We denote by $\mathbf{C}_0$ the value at $Q_0$ of the coefficient of the dimension-five operator $\mathcal{O}_5 = -\mathbf{C}_{AB}(L_A H)(L_B H)/2$ related to $\mathbf{C}(M_Z)$ directly by the RGEs of the MSSM derived in [53]. At the scale $Q_0$, we can use (3) to fix the Yukawa couplings in terms of $\mathbf{\Omega}(z)$ given by one of the three patterns (6)-(8). Once $\mathbf{Y}_\nu(Q_0)$ is determined by $\mathbf{\Omega}$, the RGEs for $\mathbf{Y}_\nu$, $M_A$ and $m_{\nu_B}$ can be used to calculate these quantities at any other scale $M_1 < Q < M_{\rm GUT}$. Indeed, one can obviously define the running of the coefficient of the $\mathcal{O}_5$ operator also for $Q \neq Q_0$, because this operator could be added to the initial Lagrangian with right-chiral neutrinos present. Above $Q_0$, the RGE for $\mathbf{C}$ is

$$\frac{d}{dt}\mathbf{C} = -K\mathbf{C} - \left[(\mathbf{Y}_e^\dagger \mathbf{Y}_e)^T + (\mathbf{Y}_\nu^\dagger \mathbf{Y}_\nu)^T\right]\mathbf{C} - \mathbf{C}\left[(\mathbf{Y}_e^\dagger \mathbf{Y}_e) + (\mathbf{Y}_\nu^\dagger \mathbf{Y}_\nu)\right], \tag{26}$$

where $K = -6g_2^2 - 2g_y^2 + 2{\rm Tr}(3\mathbf{Y}_u^\dagger \mathbf{Y}_u + \mathbf{Y}_\nu^\dagger \mathbf{Y}_\nu)$. By evolving $\mathbf{C}$ to an arbitrary scale $Q$ by using the RGE (26) with $\mathbf{C}_0$ as the initial condition at $Q_0$ [6] one can use (3) to define $\tilde{\mathbf{\Omega}}_{AB}$ at any scale $Q \neq Q_0$ by the formula

$$\tilde{\mathbf{\Omega}}_{AB} = -\frac{i}{\sqrt{M_A}}(\mathbf{O}_R \mathbf{Y}_\nu \mathbf{U}_\nu)^{AB}\frac{1}{c_B}, \tag{27}$$

where $\mathbf{U}_\nu$ diagonalizes $\mathbf{C}$ at $Q$, and $\mathbf{O}_R$ is the unitary matrix diagonalizing $M_R$ at $Q$. The question of consistency is now how much $\tilde{\mathbf{\Omega}}_{AB}$ differs from $\mathbf{\Omega}_{AB}$. In particular, $\tilde{\mathbf{\Omega}}_{AB}(Q)$ defined in this way needs not be orthogonal, because in general $\mathbf{C}(Q)$ would be numerically different from $\mathbf{Y}_\nu^T \mathbf{M}_R^{-1} \mathbf{Y}_\nu$ at the same scale.

However, it is easy to see that in supersymmetry $\tilde{\mathbf{\Omega}}_{AB}(Q)$ defined in this way *is* orthogonal because the RGE (26) is exactly the same as the RGE of the combination $\mathbf{Y}_\nu^T \mathbf{M}_R^{-1} \mathbf{Y}_\nu$, as obtained by using the chain differentiation rule and the RGEs of $\mathbf{Y}_\nu$

[6] For hierarchical light neutrino masses, the renormalization effects between the scale $M_Z$ and $Q_0$ on the mass eigenvalues and, in particular, on the mixing matrix $\mathbf{U}_\nu$ are small, and $\mathbf{C}_0$ can be identified with $\mathbf{U}_\nu^* {\rm diag}(m_{\nu_1}, m_{\nu_2}, m_{\nu_3})\mathbf{U}_\nu^\dagger$ at the electroweak scale.

and $\mathbf{M}_R$ given, e.g., in [31]. This is because, in supersymmetry, the Yukawa couplings, the right-chiral neutrino mass term and the dimension-five operator are all $F$ terms. Therefore, due to the non-renormalization theorems, the RG running of their coefficients are entirely given by the wave function renormalization of the (super)fields out of which they are built. It then follows that renormalization of the $N_A$ (super)fields, which does not enter the running of $\mathbf{C}$, also cancels out in the expression for the RGE for $\mathbf{Y}_\nu^T\mathbf{M}_R^{-1}\mathbf{Y}_\nu$.

The RGE for $\tilde{\mathbf{\Omega}}$ can be then obtained by simply differentiating the formula (27), using the known RGEs for $\mathbf{U}_\nu$ and $c_B$ [30, 31], the RGE for $\mathbf{Y}_\nu$ (see, e.g., the Appendix of [31] [7]) and the RGEs for $M_A$ and $\mathbf{O}_R$ obtained by applying the technique of [54, 30, 31] to the RGE for $\mathbf{M_R}$ derived in [55]. One then gets

$$\begin{aligned}\frac{d}{dt}M_A &= 4M_A\left[\mathbf{O}_R^\dagger(\mathbf{Y}_\nu\mathbf{Y}_\nu^\dagger)^T\mathbf{O}_R\right]^{AA}\\ \frac{d}{dt}\mathbf{O}_R^{AB} &= \sum_C \mathbf{O}_R^{AC}\varepsilon_O^{CB}\end{aligned} \tag{28}$$

where $\varepsilon_O^\dagger = -\varepsilon_O$, $\varepsilon_O^{AA} = 0$ and

$$\varepsilon_O^{AB} = -2\frac{M_A+M_B}{M_A-M_B}\mathrm{Re}\left[\mathbf{O}_R^\dagger(\mathbf{Y}_\nu\mathbf{Y}_\nu^\dagger)^T\mathbf{O}_R\right]^{AB} - 2i\frac{M_A-M_B}{M_A+M_B}\mathrm{Im}\left[\mathbf{O}_R^\dagger(\mathbf{Y}_\nu\mathbf{Y}_\nu^\dagger)^T\mathbf{O}_R\right]^{AB} \tag{29}$$

for $A \neq B$. Combining all the elements, one gets

$$\begin{aligned}\frac{d}{dt}\tilde{\mathbf{\Omega}}_{AB} &= 2\frac{M_A}{\langle H\rangle^2}\sum_{D\neq A}\sum_C\left[\frac{M_D m_{\nu_C}}{(M_D-M_A)}\mathsf{Re}\left(\tilde{\mathbf{\Omega}}_{AC}\tilde{\mathbf{\Omega}}^*_{DC}\right) + i\frac{M_D m_{\nu_C}}{(M_D+M_A)}\mathsf{Im}\left(\tilde{\mathbf{\Omega}}_{AC}\tilde{\mathbf{\Omega}}^*_{DC}\right)\right]\tilde{\mathbf{\Omega}}_{DB}\\ &+2\frac{m_{\nu_B}}{\langle H\rangle^2}\sum_{C\neq B}\sum_D\tilde{\mathbf{\Omega}}_{AC}\left[\frac{m_{\nu_C}M_D}{(m_{\nu_B}-m_{\nu_C})}\mathsf{Re}\left(\tilde{\mathbf{\Omega}}^*_{DC}\tilde{\mathbf{\Omega}}_{DB}\right) + i\frac{m_{\nu_C}M_D}{(m_{\nu_B}+m_{\nu_C})}\mathsf{Im}\left(\tilde{\mathbf{\Omega}}^*_{DC}\tilde{\mathbf{\Omega}}_{DB}\right)\right]\\ &+2\sum_{C\neq B}\sum_D\tilde{\mathbf{\Omega}}_{AC}y^2_{e_D}\left[\frac{\sqrt{m_{\nu_B}m_{\nu_C}}}{m_{\nu_B}-m_{\nu_C}}\mathsf{Re}\left(\mathbf{U}_\nu^{DC*}\mathbf{U}_\nu^{DB}\right) + i\frac{\sqrt{m_{\nu_B}m_{\nu_C}}}{m_{\nu_B}+m_{\nu_C}}\mathsf{Im}\left(\mathbf{U}_\nu^{DC*}\mathbf{U}_\nu^{DB}\right)\right]\end{aligned} \tag{30}$$

where the $y^2_{e_A}$ are the eigenvalues of $\mathbf{Y}_e^\dagger\mathbf{Y}_e$.

For non-degenerate heavy neutrinos, it is easy to see that for indices $AB$ corresponding to the small entries of $\tilde{\mathbf{\Omega}}$ in a given pattern (e.g., $\mathbf{\Omega}_{1A}$ and $\mathbf{\Omega}_{A1}$ with $A = 2, 3$ for the pattern (6)), the first two lines are small compared to 1 because they are always suppressed by the mass of the lightest left-chiral neutrino $m_{\nu_1}$. The only potentially dangerous contribution comes from $\tilde{\mathbf{\Omega}}_{AC} = 1$ in the last line. But this would require that $C = 1$, and this term is suppressed at least by a factor $\sim\sqrt{m_{\nu_1}/m_{\nu_A}}y_\tau^2$, which is also small compared to 1. Hence, for the patterns (6)-(8) $\tilde{\mathbf{\Omega}} \approx \mathbf{\Omega}$ independently of the choice of $Q_0$, if the heavy neutrinos are not degenerate.

Stability of the patterns (6)-(8) may be more problematic for arbitrarily tight degeneracy of the right-chiral neutrinos. One may, however, ask whether the pattern (8) is

[7] In the expression (B.12) of this reference the factor of 3 should multiply $\mathbf{Y}_\nu^\dagger\mathbf{Y}_\nu$ instead of $\mathbf{Y}_e^\dagger\mathbf{Y}_e$.

destabilized by the minimal degeneracy of $M_1$ and $M_2$ allowing for succesful leptogenesis with $M_1 \lesssim 10^7$ GeV [51, 38]. To make this estimate, we recall that with degenerate $M_1$ and $M_2$ the final lepton number asymmetry is roughly the same as would be obtained from decays of only one heavy neutrino having the effective mass $M_1^{\rm eff} = M_1/(M_2/M_1 - 1)$. For the pattern (8), decays of a single neutrino produce the right lepton number asymetry if its mass is $\gtrsim 10^{12}$ GeV [38]. Therefore, with the degeneracy we also need $M_1^{\rm eff} \gtrsim 10^{12}$ GeV. Consider now the contribution of the first line of (30) to the derivative of the small element $\mathbf{\Omega}_{B1}$, $B = 1, 2$. The most dangerous contribution for $A = 1$ comes from $C = 3$ and $D = 2$. It is of order $(M_1/\langle H\rangle^2)(M_2 m_{\nu_3}/(M_2 - M_1) \sim (M_1^{\rm eff} m_{\nu_3}/\langle H\rangle^2) \times \mathbf{\Omega}_{21} \ll 1$. Similarly the (nonresonant) contribution of $D = 3$ is suppressed by small $\mathbf{\Omega}_{33}$. Therefore the pattern (8) is not destabilized in this case, either.

# References


[1] Y. Fukuda *et al.* [Super-Kamiokande Collaboration], *Phys. Rev. Lett.* **81** (1998) 1562; Q. R. Ahmad *et al.* [SNO Collaboration], *Phys. Rev. Lett.* **89** (2002) 011301; K. Eguchi *et al.* [KamLAND Collaboration], *Phys. Rev. Lett.* **90** (2003) 021802

[2] F. Borzumati and A. Masiero, *Phys. Rev. Lett.* **57** (1986) 961; L.J. Hall, V.A. Kostelecky and S. Raby, *Nucl. Phys.* **B267** (1986) 415.

[3] M. Gell-Mann, P. Ramond and R. Slansky, in *Proceedings of the Supergravity Stony Brook Workshop*, New York, 1979 (eds. P. van Nieuvenhuizen and D.Z. Freedman, North-Holland, Amsterdam); T. Yanagida, in *Proceedings of the Workshop on Unified Theories and Baryon Number in the Universe*, Tsukuba, Japan, 1979 (eds. A. Sawada and A. Sugamoto, KEK Report No. 79-18, Tsukuba); R. Mohapatra and G. Senjanovic, *Phys. Rev. Lett.* **44**, 912 (1980).

[4] M. Fukugita and T. Yanagida, *Phys. Lett.* **B174** (1986) 45; M. A. Luty, *Phys. Rev.* **D45** (1992) 455.

[5] W. Buchmüller, P. Di Bari and M. Plümacher, *Nucl. Phys.* **B643** (2002) 367, *Phys. Lett.* **B547** (2002) 128, *Nucl. Phys.* **B665** (2003) 445 and preprint DESY-030100, UAB-FT-551, CERN-TH-2003-199 [arXiv:hep-ph/0401240]

[6] J. A. Casas and A. Ibarra, *Nucl.Phys.* **B618** (2001) 171

[7] S. Davidson and A. Ibarra, *JHEP* **0109** (2001) 013; J. R. Ellis, J. Hisano, M. Raidal and Y. Shimizu, *Phys. Rev.* **D66** (2002) 115013

[8] G.C. Branco, T. Morozumi, B.M. Nobre, M.N. Rebelo, *Nucl. Phys.* **B617** (2001) 475; A.S. Joshipura, E. A. Paschos, W. Rodejohann, *JHEP* **0108** (2001) 029; D. Falcone, *Phys. Rev.* **D66** (2002) 053001; G. C. Branco, R. Gonzalez Felipe, F.R. Joaquim, M.N. Rebelo, *Nucl. Phys.* **B640** (2002) 202; W. Rodejohann, *Phys. Lett.* **B542** (2002) 100; *Eur. Phys. J.* **C32** (2004) 235; E. Kh. Akhmedov, M. Frigerio, A. Yu.

Smirnov, *JHEP* **0309** (2003) 021; S. Pascoli, S. T. Petcov and W. Rodejohann, *Phys. Rev.* **D68** (2003) 093007; S. Davidson and R. Kitano, *JHEP* **0403** (2004) 020

[9] J. R. Ellis and M. Raidal, *Nucl. Phys.* **B643** (2002) 229

[10] S. Davidson, *JHEP* **0303** (2003) 037

[11] S. Davidson and A. Ibarra, *Nucl. Phys.* **B648** (2003) 345

[12] G. C. Branco *et al.*, *Phys. Rev.* **D67** (2003) 073035.

[13] A. Y. Smirnov, *Phys. Rev.* **D48** (1993) 3264; S.F. King, *Phys. Lett.* **B439** (1998) 350 and *Nucl. Phys.* **B562** (1999) 57 and *Nucl. Phys.* **B576** (2000) 85 and *JHEP* **0209** (2002) 011 and *Rept. Prog. Phys.* **67** (2004) 107; S. Davidson and S.F. King, *Phys. Lett.* **B445** (1998) 191; Q. Shafi and Z. Tavarkiladze, *Phys. Lett.* **B451** (1999) 129; G. Altarelli, F. Feruglio and I. Masina, Phys. Lett. B **472** (2000) 382; S.F. King and G.G. Ross, *Phys. Lett.* **B520** (2001) 243.

[14] For a review see, e.g., G. Altarelli and F. Feruglio, *Phys. Rept.* **320** (1999) 295 and in *Neutrino Mass*, Springer Tracts in Modern Physics, eds. G. Altarelli and K. Winter

[15] H. Murayama, H. Suzuki, T. Yanagida and J. Yokoyama, *Phys. Rev. Lett.* **70** (1993) 1912; H. Murayama, H. Suzuki, T. Yanagida and J. Yokoyama, *Phys. Rev.* **D50** (1994) 2356; K. Hamaguchi, H. Murayama and T. Yanagida, *Phys. Rev.* **D65** (2002) 043512

[16] J. R. Ellis, J. E. Kim and D. V. Nanopoulos, *Phys. Lett.* **B145** (1984) 181; J. R. Ellis, D. V. Nanopoulos and S. Sarkar, *Nucl. Phys.* **B259** (1985) 175; J. R. Ellis, D. V. Nanopoulos, K. A. Olive and S. J. Rey, *Astropart. Phys.* **4** (1996) 371; M. Kawasaki and T. Moroi, *Prog. Theor. Phys.* **93** (1995) 879; T. Moroi, Ph.D. thesis, arXiv:hep-ph/9503210; M. Bolz, A. Brandenburg and W. Buchmüller, *Nucl. Phys.* **B606** (2001) 518; R. Cyburt, J. R. Ellis, B. D. Fields and K. A. Olive, *Phys.Rev.* **D67** (2003) 103521

[17] J. R. Ellis, M. Raidal and T. Yanagida, *Phys. Lett.* **B581** (2004) 9

[18] C. L. Bennett *et al.*, *Astrophys. J. Suppl.* **148** (2003) 1; D. N. Spergel *et al.*, *Astrophys. J. Suppl.* **148** (2003) 175; H. V. Peiris *et al.*, *Astrophys. J. Suppl.* **148** (2003) 213

[19] G. Lazarides, Q. Shafi, *Phys. Lett.* **B258** (1991) 305.

[20] J. Hisano, T. Moroi, K. Tobe, M. Yamaguchi and T. Yanagida, *Phys. Lett.* **B357** (1995) 579; J. Hisano, T. Moroi, K. Tobe and M. Yamaguchi, *Phys. Rev.* **D53** (1996) 2442; J. Hisano and D. Nomura, *Phys. Rev.* **D59** (1999) 116005.

[21] X. J. Bi, B. Feng and X. M. Zhang, [arXiv:hep-ph/0309195].

[22] T. Blažek and S. F. King, *Nucl. Phys.* **B662** (2003) 359

[23] J. R. Ellis, J. Hisano, S. Lola and M. Raidal, *Nucl. Phys.* **B621** (2002) 208

[24] S. Lavignac, I. Masina and C. A. Savoy, *Phys. Lett.* **B520** (2001) 269 and *Nucl. Phys.* **B633** (2002) 139

[25] S. Pascoli, S. T. Petcov and C. E. Yaguna, *Phys. Lett.* **B564** (2003) 241; S. T. Petcov, S. Profumo, Y. Takanishi and C. E. Yaguna, *Nucl. Phys.* **B676** (2004) 453

[26] A. Ibarra and G. G. Ross, preprint CERN-TH-2003-294, [arXiv:hep-ph/0312138].

[27] K. Tobe, J. D. Wells and T. Yanagida, *Phys. Rev.* **D69** (2004) 035010

[28] A. Masiero, S. Profumo, S. K. Vempati and C. E. Yaguna, *JHEP* **0403** (2004) 046

[29] B. A. Campbell, D. W. Maybury and B. Murakami, *JHEP* **0403** (2004) 052

[30] P. H. Chankowski, W. Królikowski and S. Pokorski, *Phys. Lett.* **B473** (2000) 109; J. A. Casas, J. R. Espinosa, A. Ibarra and I. Navarro, *Nucl. Phys.* **B573** (2000) 652.

[31] P. H. Chankowski and S. Pokorski, *Int. J. Mod. Phys.* **A17** (2002) 575

[32] P. H. Frampton, S. L. Glashow and T. Yanagida, *Phys. Lett.* **B548** (2002) 119; M. Raidal and A. Strumia, *Phys. Lett.* **B553** (2003) 72; S. F. King, *Phys. Rev.* **D67** (2003) 113010; S. Raby, *Phys. Lett.* **B561** (2003) 119; B. Dutta and R. N. Mohapatra, *Phys. Rev.* **D68** (2003) 056006; V. Barger, D. A. Dicus, H. J. He and T. j. Li, *Phys. Lett.* **B583** (2004) 173; W. l. Guo and Z. z. Xing, *Phys. Lett.* **B583** (2004) 163

[33] R. Barbieri, T. Hambye and A. Romanino, *JHEP* **0303** (2003) 017

[34] R. Kuchimanchi and R. N. Mohapatra, *Phys. Rev.***D66** (2002) 051301; R. Kuchimanchi and R. N. Mohapatra, *Phys. Lett.* **B552** (2003) 198

[35] G. Altarelli and F. Feruglio, *Phys. Lett.* **B451** (1999) 388

[36] Y. Grossman, Y. Nir and Y. Shadmi, *JHEP* **9810** (1998) 007; Y. Nir and Y. Shadmi, *JHEP* **9905** (1999) 023; J. Feng, Y. Nir and Y. Shadmi, *Phys. Rev.* **D61** (2000) 113005.

[37] M. Hirsch and S. F. King, *Phys. Rev.* **D64** (2001) 113005

[38] P. H. Chankowski and K. Turzyński, *Phys. Lett.* **B570** (2003) 198

[39] A. Ibarra and G. G. Ross, *Phys. Lett.* **B575** (2003) 279

[40] M. Y. Khlopov and A. D. Linde, *Phys. Lett.* **B138** (1984) 265; I. V. Falomkin *et al. Nuovo Cim.* **A79** (1984) 193 [*Yad. Fiz.* **39** (1984) 990]; M. Y. Khlopov, Y. L. Levitan, E. V. Sedelnikov and I. M. Sobol, *Yad. Fiz.* **57** (1994) 1466; K. Kohri *Phys. Rev.* **D64** (2001) 043515; M. Kawasaki, K. Kohri and T. Moroi, preprint RESCEU-04-04 [arXiv:astro-ph/0402490].

[41] J. R. Ellis, K. A. Olive, Y. Santoso and V. C. Spanos, *Phys. Lett.* **B565** (2003) 176; preprint CERN-TH-2003-310 [arXiv:hep-ph/0312262].

[42] J. R. Ellis, J. Hisano, M. Raidal and Y. Shimizu, *Phys. Lett.* **B528** (2002) 86

[43] S. Davidson and A. Ibarra, *Phys. Lett.* **B535** (2002) 25

[44] T. Hambye, Y. Lin, A. Notari, M. Papucci and A. Strumia, preprint FUP-TH-2003-48 [arXiv:hep-ph/0312203]

[45] G. F. Giudice, A. Notari, M. Raidal, A. Riotto and A. Strumia, preprint CERN-TH-2003-240 [arXiv:hep-ph/0310123].

[46] L. Covi, E. Roulet and F. Vissani, *Phys. Lett.* **B384** (1996) 169; A. Pilaftsis, *Int. J. Mod. Phys.* **A14** (1999) 1811

[47] M. Fujii, M. Ibe and T. Yanagida, *Phys. Lett.* **B579** (2004) 6

[48] M. Flanz, E. A. Paschos and U. Sarkar, *Phys. Lett.* **B345** (1995) 248, Erratum - *ibid.* **B382** (1996) 447; M. Flanz, E. A. Paschos, U. Sarkar and J. Weiss, *Phys. Lett.* **B389** (1996) 693

[49] A. Pilaftsis and T. E. Underwood, preprint MC-TH-2003-09 [arXiv:hep-ph/0309342].

[50] R. Gonzalez Felipe, F. R. Joaquim and B. M. Nobre, arXiv:hep-ph/0311029.

[51] J. R. Ellis, M. Raidal and T. Yanagida, *Phys. Lett.* **B546** (2002) 228.

[52] K. Turzynski, preprint IFT-04/05 [arXiv:hep-ph/0401219].

[53] P. H. Chankowski and Z. Płuciennik, *Phys. Lett.* **B316** (1993) 312; K. S. Babu, C. N. Leung and J. Pantaleone, *Phys. Lett.* **B319** (1993) 191.

[54] K. S. Babu, *Z. Phys.* **C35** (1987) 69.

[55] J. A. Casas, J. R. Espinosa, A. Ibarra and I. Navarro, *Nucl.Phys.* **B569** (2000) 82.

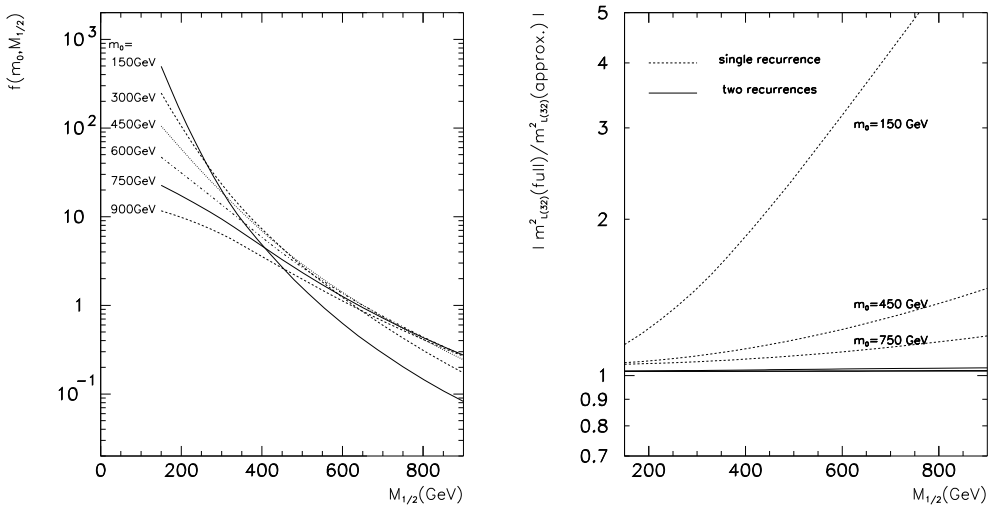


Figure 1: *Left panel:* $f(m_0, M_{1/2}) \equiv \mathcal{F}(m_0, M_{1/2})/\mathcal{F}(100\,\mathrm{GeV}, 500\,\mathrm{GeV})$ *as a function of* $M_{1/2}$ *for* $\tan\beta = 10$ *and* $\mu > 0$. *The normalization is such that* $f(m_0, M_{1/2}) = 1$ *for* $m_0 = 100$ *GeV,* $M_{1/2} = 500$ *GeV, consistent with the dark matter constraints [41]. Right panel: The ratio of* $\tilde{\mathbf{m}}^2_{L_{32}}(\mathsf{full})$ *obtained by numerical integration of the full set of the RGEs to* $\tilde{\mathbf{m}}^2_{L_{32}}(\mathsf{approx.})$ *obtained with the use of the formula (15) as a function of* $M_{1/2}$ *for* $\tan\beta = 10$ *and* $A_0 = 0$.

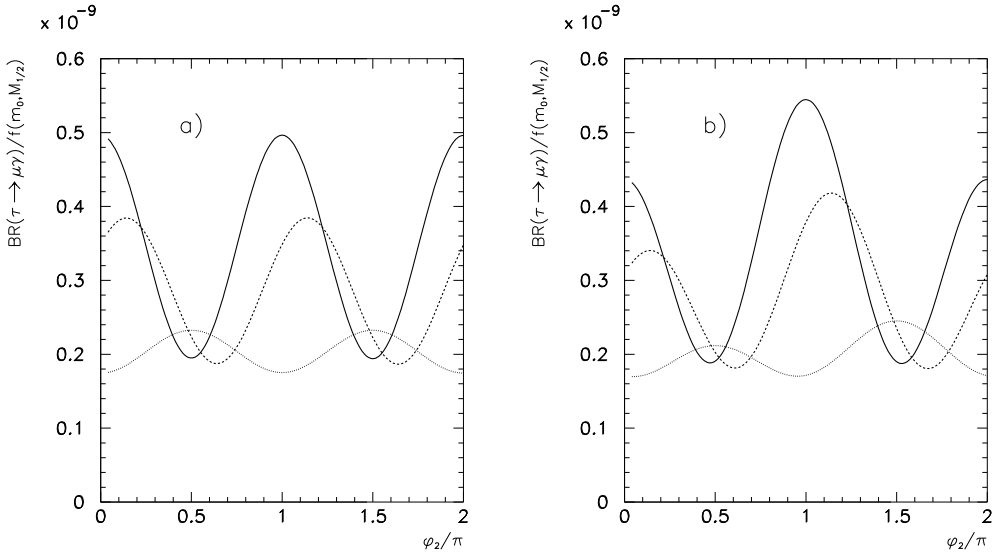


Figure 2: $BR(\tau \to \mu\gamma)/f(m_0, M_{1/2})$ *as a function of* $\phi_2$ *for the choice of the remaining phases described in Table 1,* $|z| = 1/\sqrt{2}$, $\tan\beta = 10$ *and* $A_0 = 0$. *Dotted, dashed and solid lines correspond to* $\arg z = 0, \pi/4, \pi/2$, *respectively.*

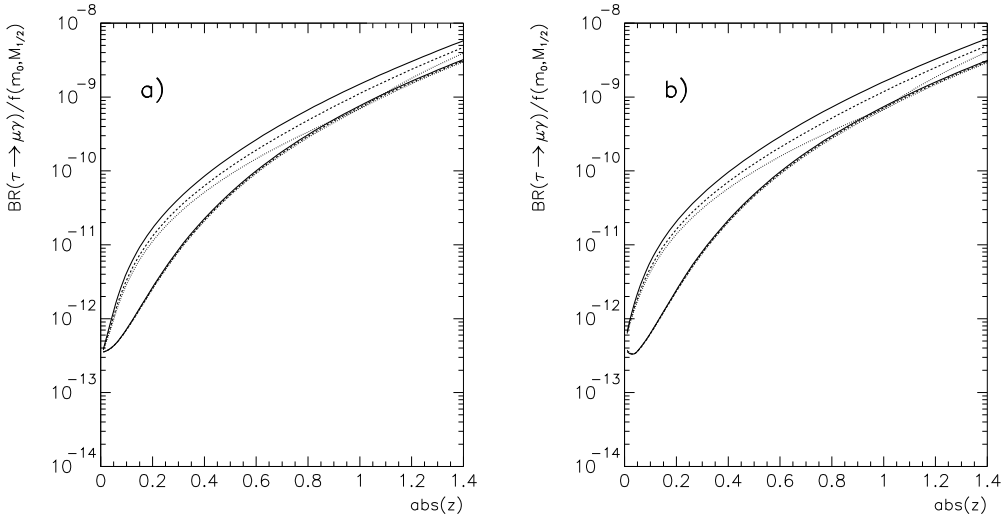


Figure 3: *Extremal values of* $BR(\tau \to \mu\gamma)/f(m_0, M_{1/2})$ *as a function of* $|z|$ *for the choice of the parameters described in Table 1,* $\tan\beta = 10$ *and* $A_0 = 0$*. Dotted, dashed and solid lines correspond to* $\arg z = 0, \pi/4, \pi/2$*, respectively.*

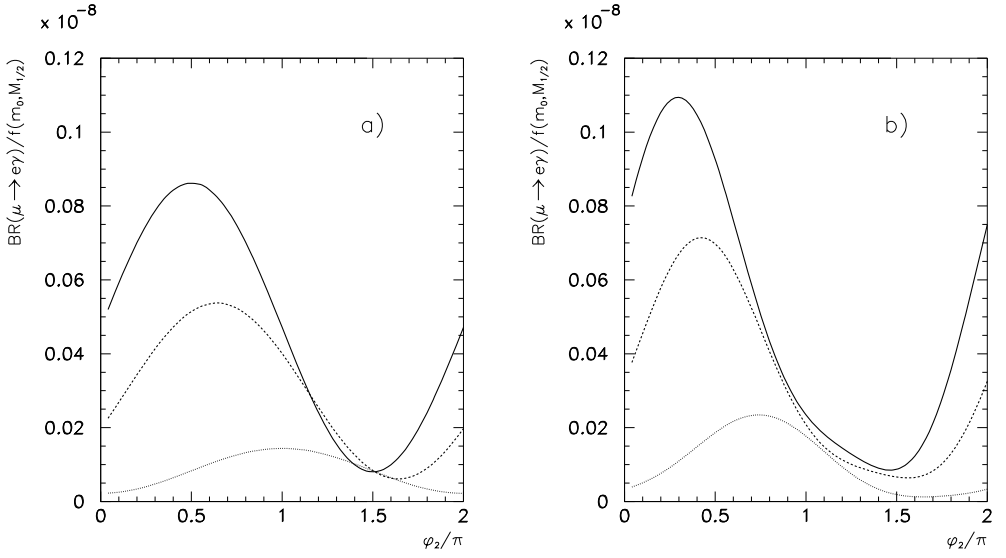


Figure 4: $BR(\mu \to e\gamma)/f(m_0, M_{1/2})$ *as a function of* $\phi_2$ *for the choice of the remaining phases described in Table 1,* $|z| = 1/\sqrt{2}$*,* $\tan\beta = 10$ *and* $A_0 = 0$*. Dotted, dashed and solid lines correspond to* $\arg z = 0$*,* $\pi/4$ *and* $\pi/2$*, respectively.*

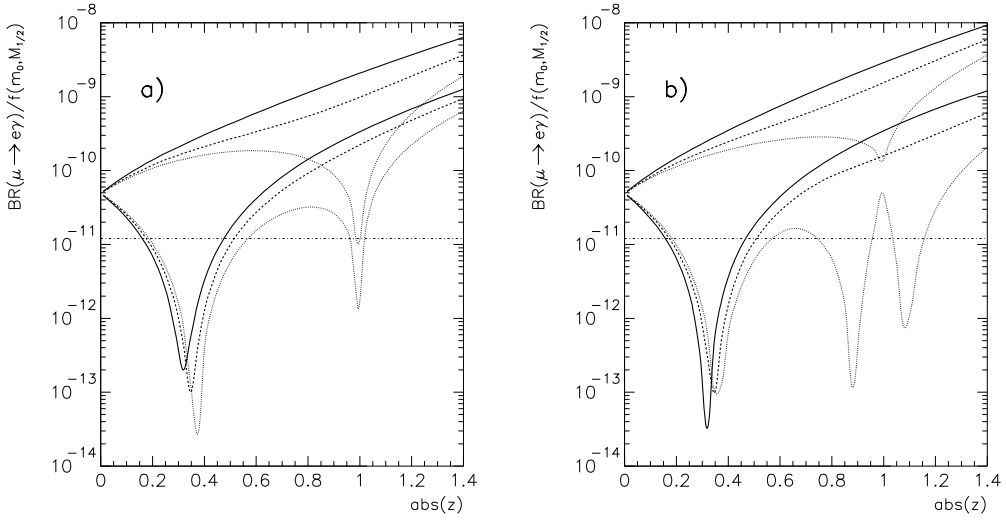


Figure 5: *Extremal values of* $BR(\mu \to e\gamma)/f(m_0, M_{1/2})$ *as a function of* $|z|$ *for the choice of the parameters described in Table 1,* $\tan\beta = 10$ *and* $A_0 = 0$*. Dotted, dashed and solid lines correspond to* $\arg z = 0$*,* $\pi/4$ *and* $\pi/2$*, respectively.*

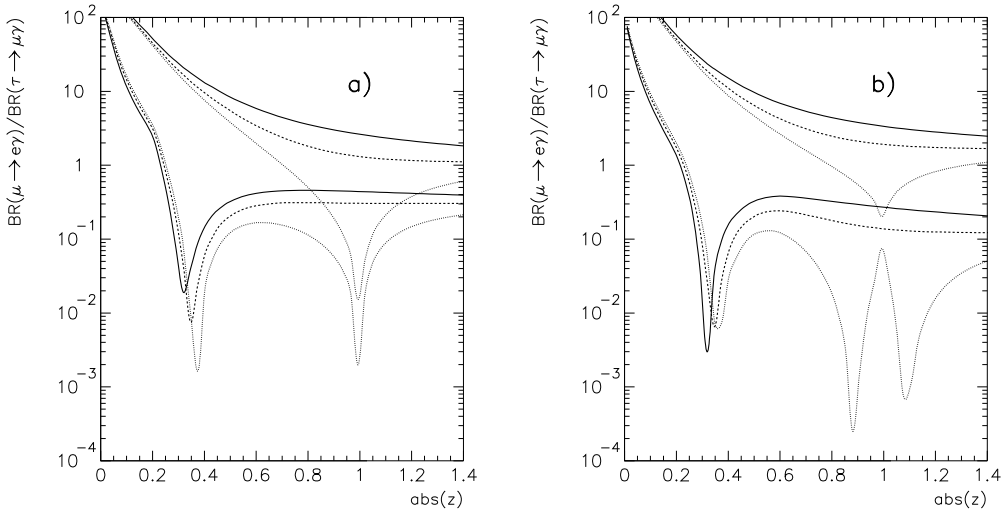


Figure 6: *Extremal values of* $BR(\mu \to e\gamma)/BR(\tau \to \mu\gamma)$ *as a function of* $|z|$ *for the choice of the parameters described in Table 1. Dotted, dashed and solid lines correspond to* $\arg z = 0$*,* $\pi/4$ *and* $\pi/2$*, respectively.*

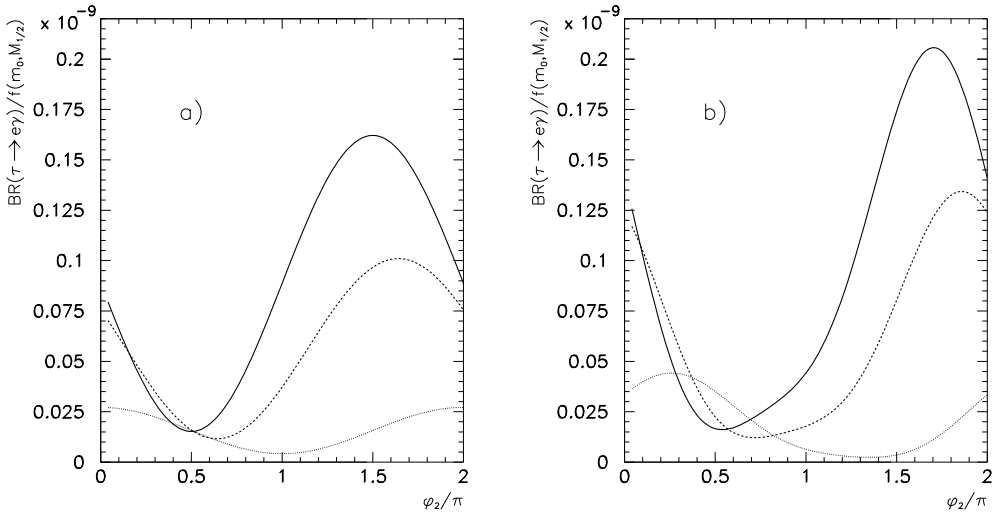


Figure 7: *$BR(\tau \to e\gamma)$ as a function of $\phi_2$ for the choice of the remaining phases described in Table 1, $|z| = 1/\sqrt{2}$, $\tan\beta = 10$ and $A_0 = 0$. Dotted, dashed and solid lines correspond to $\arg z = 0$, $\pi/4$ and $\pi/2$, respectively.*

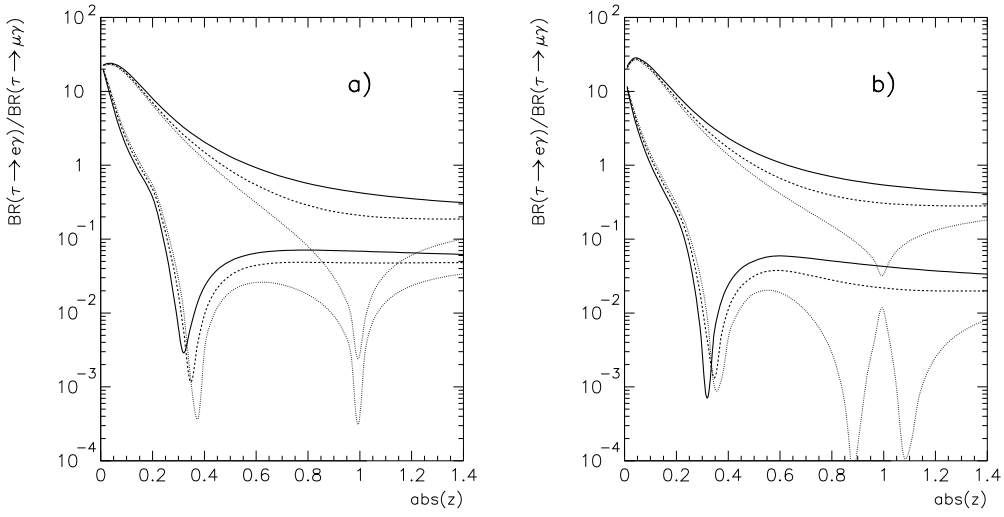


Figure 8: *The extremal values of $BR(\tau \to e\gamma)/BR(\tau \to \mu\gamma)$ as a function of $|z|$ for the choice of the parameters described in Table 1, $\tan\beta = 10$ and $A_0 = 0$. Dotted, dashed and solid lines correspond to $\arg z = 0$, $\pi/4$ and $\pi/2$, respectively.*

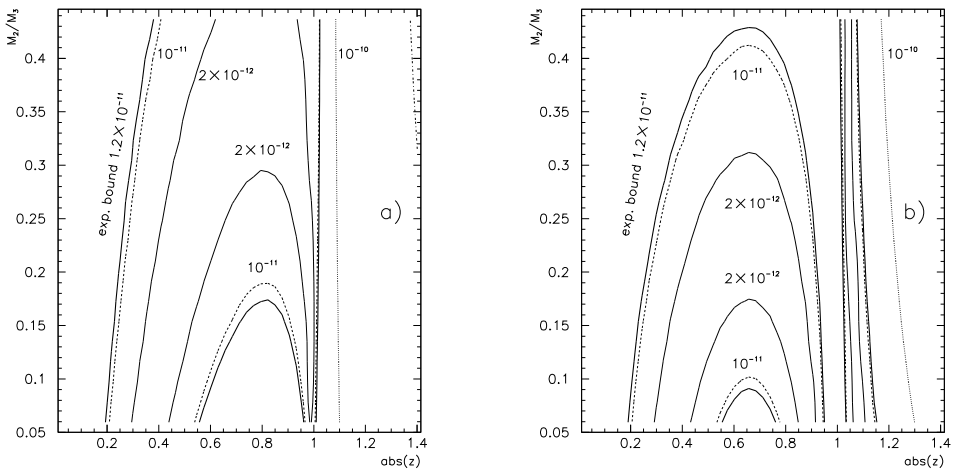


Figure 9: *Contour plot of* $BR(\mu \to e\gamma)/f(m_0, M_{1/2})$ *minimized with respect to the variation of* $\phi_2$ *as a function of* $|z|$ *and* $M_2/M_3$ *for the choice of the parameters described in Table 1,* $\tan\beta = 10$*,* $A_0 = 0$ *and* $\arg z = 0$*.*

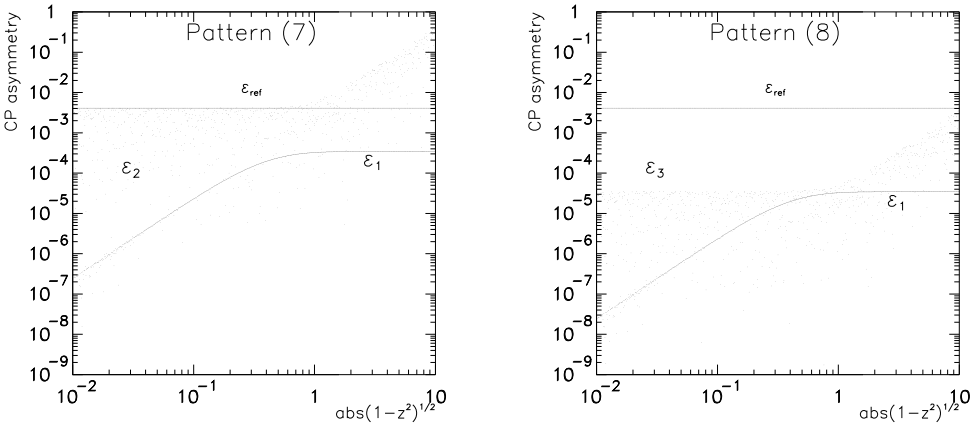


Figure 10: *The CP asymmetries generated in the decays of the sneutrino-inflaton for the pattern (7) (left panel) and (8) (right panel). Details of the scanning procedure are given in the text.*

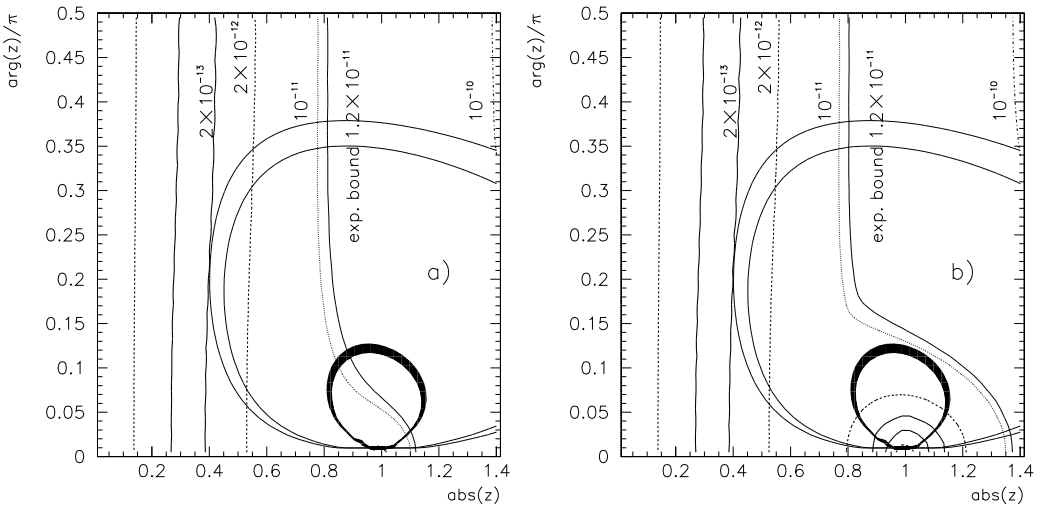


Figure 11: *Minimal values of* $BR(\mu \to e\gamma)/f(m_0, M_{1/2})$ *for* $\tan\beta = 10$ *and* $A_0 = 0$. *The dark ring is the region of* $z$ *in the complex plane for which leptogenesis is successful for* $M_1 = 10^{11}$ *GeV. The larger ring bounded by thin solid lines show how this region changes for* $M_1 = 5 \times 10^{11}$ *GeV.*